THE JOURNAL OF PHYSICAL CHEMISTRY A

ARTICLE

pubs.acs.org/JPCA

Conformational Structure of Tyrosine, Tyrosyl-glycine, and Tyrosyl-glycyl-glycine by Double Resonance Spectroscopy

Ali Abo-Riziq,[†,§] Louis Grace,[†,∥] Bridgit Crews,[†,⊥] Michael P. Callahan,[†,#] Tanja van Mourik,[‡] and Mattanjah S. de Vries[†,*]

[†]Department of Chemistry and Biochemistry, University of California, Santa Barbara, California 93106, United States

[‡]EaStCHEM School of Chemistry, University of St. Andrews North Haugh, St. Andrews, Fife KY16 9ST, Scotland, U.K.

ABSTRACT: We investigated the variation in conformation for the amino acid tyrosine (Y), alone and in the small peptides tyrosine-glycine (YG) and tyrosine-glycine-glycine (YGG), in the gas phase by using UV−UV and IR−UV double resonance spectroscopy and density functional theory calculations. For tyrosine we found seven different conformations, for YG we found four different conformations, and for YGG we found three different conformations. As the peptides get larger, we observe fewer stable conformers, despite the increasing complexity and number of degrees of freedom. We find structural trends similar to those in phenylalanine-glycine-glycine (FGG) and tryptophan-glycine-glycine (WGG); however, the effect of dispersive forces in FGG for stabilizing a folded structure is replaced by that of hydrogen bonding in YGG.

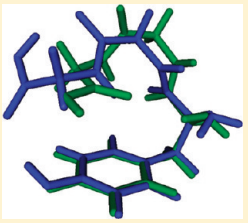

1. INTRODUCTION

Small peptides can provide useful models for studying the forces responsible for the structure and activity of larger proteins. In the gas phase we can isolate these molecules and study them free of solvent interactions, or simulate their behavior in solution by producing clusters with different solvent molecules.[1−3] One approach is to study small peptide sections by "protecting" the ends with groups that eliminate the functionality of the N and C terminus.[4−6] Alternatively, by studying actual unprotected short sequences, we can examine the structural role played by the termini.[7−11]

To perform resonant two-photon ionization (R2PI) and double resonance spectroscopy (or hole burning spectroscopy), any molecule we study must contain a chromophore. The three amino acids that contain suitable chromophores are phenylalanine,[12] tryptophan,[13−16] and tyrosine.[17,18] A number of studies have been reported on small peptides containing phenylalanine and tryptophan. Mons et al. studied protected small peptides containing phenylalanine as a model for protein segments.[6,19,20] Gerhard et al. studied clusters of protected small peptides as a model for the β-sheet form.[21−23] Kleinermanns et al. performed an intensive study of unprotected small peptides containing tryptophan.[24,25] By performing UV−UV and IR−UV double resonance spectroscopy on tryptophan-glycine (WG) and tryptophan-glycine-glycine (WGG), they found that the number of conformations decreased for the di- and tripeptides compared to that for the single amino acid. They saw this as evidence that as peptides increase in size the conformational space available to them decreases, and they proposed further work to determine whether this provides the means for large peptides to relax to their global minima.[24−26] This explanation was also supported by research conducted in our group on larger molecules, where we observed single conformers for both penta- and hexapeptides and for peptides containing up to 15 amino acid residues.[8] In our group, we are studying unprotected small and large peptides containing either phenylalanine or tyrosine. The reason for selecting these chromophores is that the only difference between these two amino acids is the hydroxyl on the phenyl group of the tyrosine. Previously, we studied di- and tripeptides containing phenylalanine. Calculations by Řeha et al. showed that for phenylalanine-glycine-glycine (FGG), dispersion forces were the dominant forces in determining the structure. The carboxylic group, in this case, folds back to a position above the benzene ring of the phenylalanine. To identify this structure, it was necessary to perform a new type of calculation that properly estimates these forces.[10]

The gas phase spectroscopy of tyrosine (Y) has been extensively studied by various groups. Martinez et al. were the first to assign the origin bands in the UV spectrum of tyrosine, which they obtained by laser-induced fluorescence.[18] By examining the relative intensities of the peaks in the origin region as a function of laser power, they identified 10 different conformers. In Lubman's group[27,28] and in our group[29] we studied the R2PI spectrum of tyrosine, and we obtained a spectrum similar to that of Martinez et al.[30] All these spectra exhibited doublets with spacings of about 5 cm^{-1}. These doublets were assigned as origins of conformers that differ in the orientation of the hydroxyl on the phenolic ring. In this work we show that the origin spacing for some conformer pairs (that differ only in the orientation of the ring hydroxyl group) is about 5 cm^{-1}. However, the spacing for other conformer pairs is much greater and is on the order of 30 cm^{-1}. This necessitates a slight modification of our earlier assignment. In addition, the newer hole-burning results show that three peaks we had previously assigned as origin bands are actually torsions. Computationally we have studied FGG as a model for the treatment of dispersive interactions involving the π system on the ring.[10] Valdes et al. apply the same treatment to WGG[31] for which

Special Issue: Victoria Buch Memorial

Received: November 5, 2010
Revised: February 4, 2011
Published: March 17, 2011

Cable et al. already predicted a folded conformation,[32] which was confirmed in double resonant experiments by Kleinermanns and coworkers.[24,26] Toroz and van Mourik treated YG and YGG in great detail showing that for YGG dispersive interactions play a smaller role than in the FGG analogue because of the strong hydrogen bonding of the OH in the tyrosine which is absent in phenylalanine.[33]

In this paper, we present our study on tyrosine (Y), tyrosine-glycine (YG) and tyrosine-glycine-glycine (YGG). By comparing the structures we obtained with those found earlier for WGG and for FGG, we can evaluate the role played by this aromatic amino acid, and of its hydroxyl group. The tyrosine functional group is particularly important in folded structures in which this group interacts with the C terminus. We also discuss the issue of the decrease in the number of conformations as the size of the peptide increases. We note that the tripeptide is the smallest sequence that can fold in a way that allows the C terminus to fully interact with the aromatic group.

2. METHODS

2.1. Experimental Methods. We laser desorb a mixture of pure compound from a graphite substrate with a Nd:YAG laser (1064 nm, ~10 ns pulse duration, less than 1 mJ/pulse), after which the molecules become entrained into a pulsed supersonic jet of Argon (backing pressure 6 atm). Using mass selected spectroscopy, we measure R2PI by detecting positive ions in a reflectron time-of-flight mass spectrometer.[34] In UV−UV double resonance experiments, two laser pulses are separated in time by about 200 ns. The first pulse serves as a "burn" pulse, which removes ground state population and causes depletion in the ion signal of the second "probe" pulse, provided both lasers are tuned to a resonance of the same isomer. In IR−UV double resonance spectra, the burn laser operates in the near-IR region. IR frequencies ranging from 3100 cm^{-1} to 3800 cm^{-1} are produced in an OPO/OPA setup (LaserVision) pumped by a Nd:YAG laser at 1064 nm. Typical IR intensities in the burn region are 8−10 mJ $pulse^{-1}$ with a bandwidth of 3 cm^{-1}. The resulting ion-dip spectra are ground-state IR spectra that are optically selected by means of the probe laser R2PI wavelength and mass selected by virtue of the mass spectrometer detection.

2.2. Theoretical Methods. We performed calculations on the neutral amino acid tyrosine and the di- and tripeptides YG and YGG by a two-step approach. We first used a simple molecular mechanics force field to calculate candidate structures, and then performed geometry optimization with density functional theory (DFT). We used the AMBER force field, as implemented in the AMBER7 program suite, to perform simulated annealing on each molecule. We then selected around 100 low energy candidate structures for tyrosine and 200 for the di- and tripeptides from AMBER, which were then used as starting structures for subsequent optimization with the B3LYP hybrid density functional by the program Gaussian03.

We built the preliminary structures of the molecules with the xleap program of AMBER7. We then modified the default zwitterion structure to the neutral (gas phase) structure. These structures were minimized in Gaussian03 by means of the B3LYP functional and the 6-31G* basis set. We then used the *antechamber* program of AMBER7 to generate charges from the Gaussian03 output. The charges were calculated only for a single conformation, but they were used only to calculate candidate structures by simulated annealing. We performed simulated annealing by using a simple protocol of running at high temperature (800 K) for 30 ps followed by 10 ps of (linear) cooling, and a final energy minimization. We typically repeated this cycle 500 times, sorted the results by energy, and classified them according to structure.

For tyrosine, we chose approximately 100 lowest energy candidate structures for subsequent optimization in Guassian03. We minimized

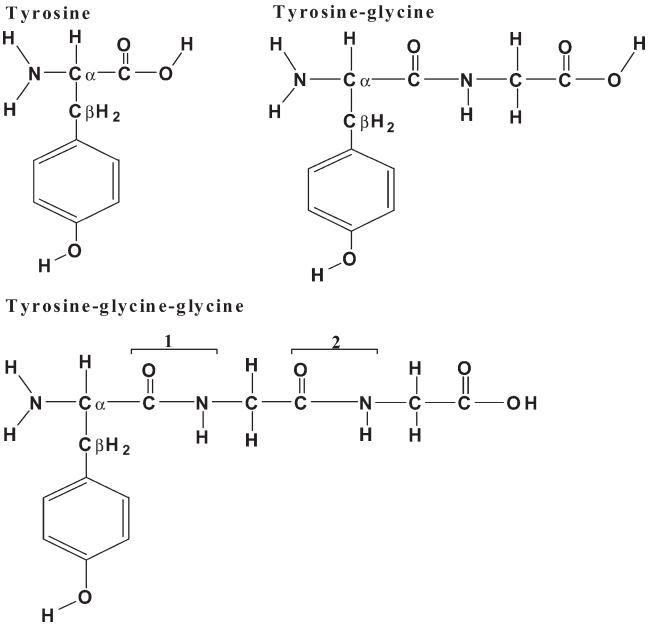

Figure 1. Structures of tyrosine, YG and YGG. The number designation for each peptide bond appears over a bracket above the bond.

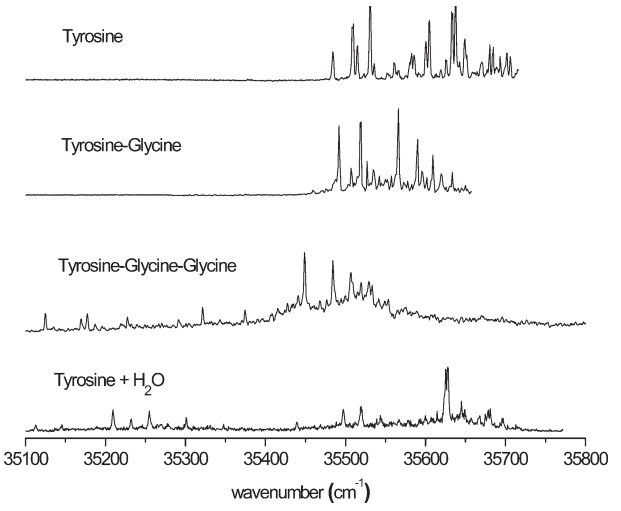

Figure 2. R2PI spectra of tyrosine (A), YG (B), YGG (C), and the cluster of tyrosine with one water molecule (D).

these with the B3LYP density functional and the 6-31G* basis set. From the resulting structures, we chose 30 candidates for optimization with a higher basis set (6-31G**). For YG we optimized the 60 lowest energy structures, and for YGG we optimized the 80 lowest energy structures, all at the 6-31G** level. As a final step, we calculated the normal-mode frequencies of all of these structures for comparison with the experimental IR obtained by IR−UV double resonance spectroscopy. The calculated frequencies were scaled by a factor of 0.9602.

3. RESULTS

Figure 1 shows the primary structures for tyrosine, YG and YGG. The α and β carbons in each structure are labeled, and the numbering of the peptide bonds in YGG is indicated by the numerals "1" and "2", each with a bracket over the appropriate bond.

Figure 2 shows the R2PI spectra of four different molecules. Spectrum A is from tyrosine. Spectrum B belongs to the dipeptide

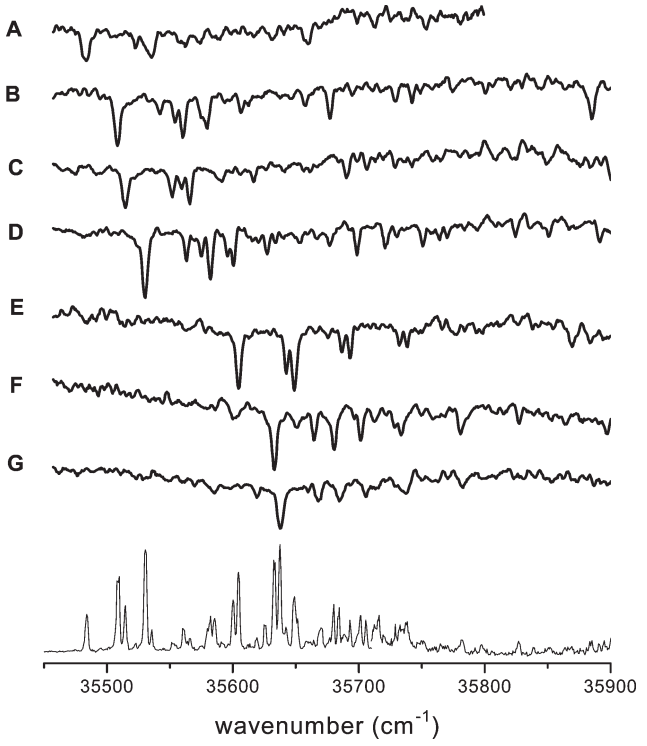

Figure 3. R2PI spectrum of tyrosine (bottom) and the UV−UV double resonance spectra for seven different conformers of tyrosine.

YG. We observe that the origins for tyrosine and for YG appear in similar frequency ranges. Spectrum C is from YGG. In addition to the cluster of peaks that appear in the same region as the origin bands for tyrosine and for YG, there is a new set of bands lower in energy (to the red). The red-most peak in this region appears about 360 cm^{-1} to the red, compared to the red-most peak in the tyrosine spectrum. As we will discuss below, we find that the peaks in this region arise from conformers in which the hydroxyl group of the phenolic ring is hydrogen bonded. The carboxylic group is folded back over the ring and interacts with the ring hydroxyl group. For comparison, spectrum D shows the R2PI spectrum for the cluster of tyrosine with one water molecule. In this cluster, one possible way for the water to interact with the tyrosine is with the hydroxyl of the phenolic ring. The R2PI spectrum of this cluster is similar to that of YGG, in that it also exhibits a group of relatively weak bands to the red of a second group of stronger peaks, presumably due to the same hydrogen bond shifts.

I. Tyrosine. Figure 3 shows the R2PI spectrum and UV−UV double resonance spectra of tyrosine. The bottom trace is the R2PI spectrum, and traces A−G are the UV−UV double resonance spectra recorded with the probe laser tuned to an intense transition of each conformer. The red-most peak in each spectrum is the origin for that conformer. We found seven different conformations (A−G) for tyrosine.

By aligning the spectra with each other, that is, by placing their origin bands one over the other, we notice that for the pairs (A,C), (B,D), and (F,G), the vibronic spectra are identical. Spectrum E does not correspond to any of the others. One possible interpretation for this, which we will discuss more fully below, is that (A,C), (B,D), and (F,G) belong to pairs of conformers in which the hydroxyl group on the ring can have two orientations, and spectrum E belongs to a conformer for which either the hydroxyl group has only one orientation or the origins arising from the two different orientations

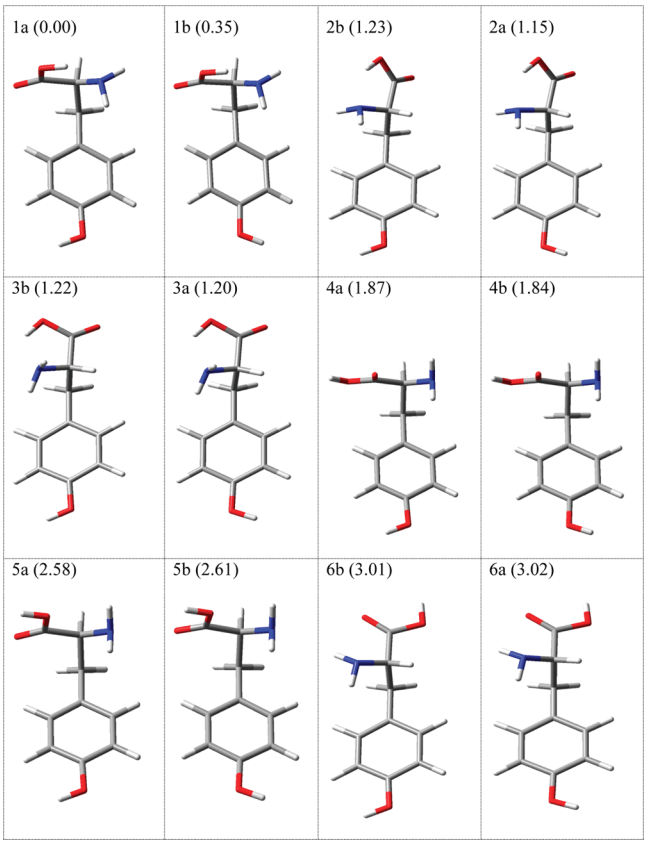

Figure 4. Lowest-energy structures of tyrosine as calculated by DFT (6-31G**). The relative energy in kcal/mol is listed above each structure.

are too close in frequency to be resolved. The former of these two possibilities may be less likely because the side chain of the tyrosine is too short to exhibit hydrogen bonding with the hydroxyl on the ring. On the other hand, it may be able to interact with the π system of the ring in such a way as to alter the electronic structure so that the orientation of the hydroxyl group is constrained.

Figure 4 shows the 12 most stable structures obtained by DFT (6-31G**). These 12 structures may be grouped into six pairs. In each pair, the only difference is the orientation of the hydroxyl group on the phenolic ring. In structures 1a and 1b, which are the most stable structures, the hydroxyl of the carboxylic group is hydrogen bonded to the lone electron pair of the nitrogen of the amino group. Structures 2a and 2b are very similar to the first pair, but with a different orientation of the amino acid backbone about the C_α-C_β bond. For structures 3a and 3b, in addition to the hydrogen bonding between the carboxylic group and the amine, one of the hydrogens of the amino group is involved in a somewhat weaker electrostatic interaction with the π-system of the aromatic ring. For structures 4a and 4b, we observe an electrostatic interaction between the oxygen of the carbonyl and both hydrogens of the amino group, and, within the carboxyl group, between the hydroxyl and the oxygen of the carbonyl. Structures 5a and 5b are very similar to the pair 4a and 4b, except that a 180° rotation of the carboxylic group leads to an electrostatic interaction between the oxygen of the hydroxyl and the hydrogens of the amine. In structures 6a and 6b, we observe an electrostatic interaction between the hydroxyl and the carbonyl, and in addition to that, an interaction between one hydrogen of the amino group and the π-system of the aromatic ring. The various

dx.doi.org/10.1021/jp110601w |J. Phys. Chem. A 2011, 115, 6077–6087

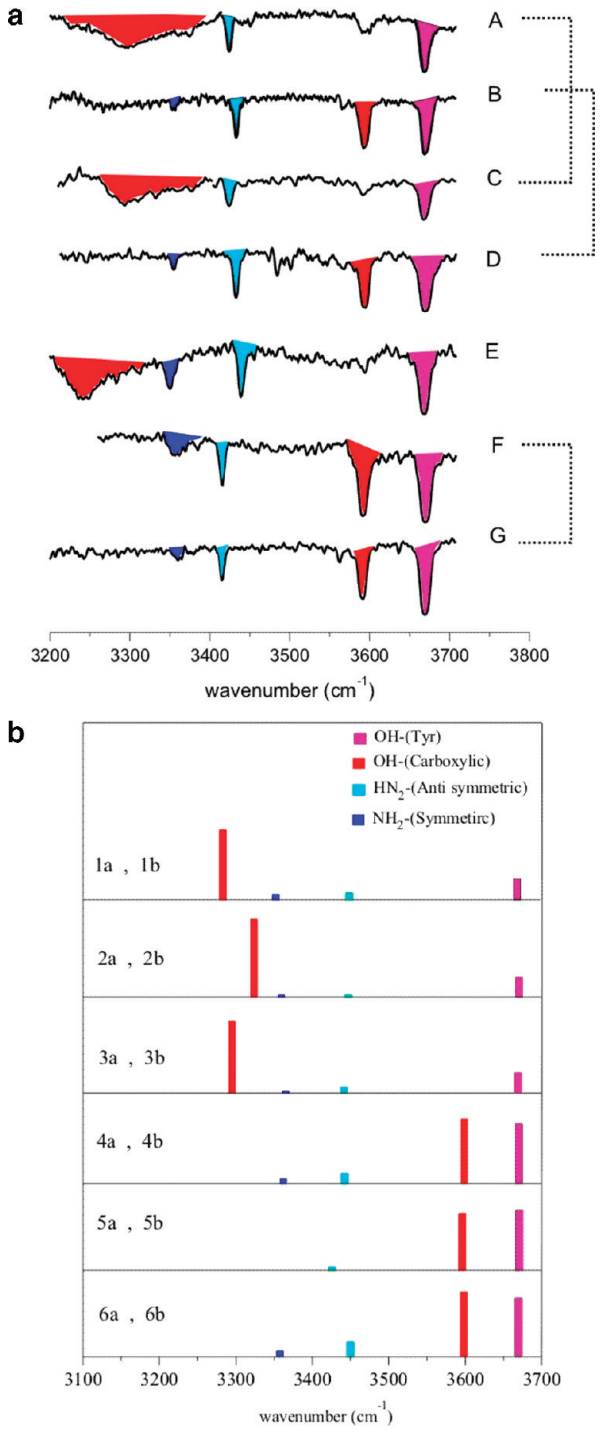

Figure 5. (a) The IR−UV double resonance spectra for the seven conformers of tyrosine observed by UV−UV double resonance spectroscopy in Figure 3. Peaks are color coded according to assignments as discussed in the text. Color coding is identical to that in panel b. (b) The calculated spectra for the 12 structures of tyrosine from Figure 4. The frequencies were scaled by a factor of 0.9602.

interactions we describe above are similar to those found by Snoek et al. for phenylalanine.[14,35]

Figure 5a shows the IR−UV double resonance spectra obtained for all seven conformers (A−G) of tyrosine found by UV−UV double resonance spectroscopy. Figure 5b shows the calculated frequencies for the 12 structures shown in Figure 4. For each pair of conformers with identical UV spectra, the experimental IR spectra are also identical. Therefore, we cannot determine the orientation of the phenolic hydroxyl for each conformer in a given pair by IR−UV double resonance spectroscopy. We can, however, determine the rest of the structure by comparing the frequencies of the calculated structures with the experimental frequencies. We identify two types of structures: (1) those with a free carboxylic OH stretch at about 3600 cm^{-1} (experimental pairs (B,D) and (F,G) and calculated pairs 4, 5, and 6) and (2) those with a hydrogen bonded carboxylic OH stretch, red-shifted to below 3200 cm^{-1} (experimental pair (A,C) and trace E and calculated pairs 1, 2, and 3). The small signal in these three traces at about 3600 cm^{-1} is possibly due to insufficient conformational selection by the probe laser.

Within each of those two groups there are three calculated pairs of structures and the precise assignment from among those structures is more tentative. For all the conformers, we found a peak at around 3669 cm^{-1}, which belongs to the free hydroxyl group on the phenolic ring. Since this frequency is not shifted, it appears the side chain of the tyrosine is not long enough to allow the carboxylic group to interact with the hydroxyl of the ring. For the first pair of spectra (A and C), the carboxylic hydroxyl group is hydrogen bonded: we observe a very broad peak whose maximum is at 3294 cm^{-1}. There are two candidate pairs of conformers: the 2a,b and 3a,b. For the first pair, we calculate the COOH frequency as 3324 cm^{-1}, while for the second pair we calculate 3294 cm^{-1}, with the 3a,b pair providing a slightly better match. The phenolic hydroxyl stretch calculated for both pairs matches very well with the experimental value of 3668 cm^{-1}. For the NH_2 antisymmetric stretch, the frequency for the first pair (2a,2b) is off by 22 cm^{-1} to the red, while for the second pair (3a,3b) it is off by 18 cm^{-1} to the red. In addition, the calculated intensity of this band for the second pair matches the experimental data somewhat better than does that calculated for the first pair. We observe the NH_2 symmetric stretch experimentally at 3376 cm^{-1}, while the calculated frequencies are 3356 cm^{-1} for the first pair and 3365 cm^{-1} for the second pair. On the basis of these observations, we tentatively assign spectra A and C to the calculated structures 3a and 3b.

Next we consider spectra B and D. These spectra exhibit intense, sharp peaks both at 3668 cm^{-1} and 3593 cm^{-1}, which indicates that both hydroxyl groups are free. The peak to the blue in both conformers belongs to the phenolic hydroxyl, while the peak to the red belongs to the carboxylic hydroxyl. Pairs 4, 5, and 6 are all possible matches, and of these the calculated frequencies and intensities for structures 6a and 6b have a slightly better fit to this pair of spectra. The NH_2 antisymmetric stretch appears at 3434 cm^{-1}, while the calculated frequency is 3450 cm^{-1}, and for the NH_2 symmetric stretch these frequencies are 3355 cm^{-1} and 3357 cm^{-1}, respectively.

For spectrum E we did not observe another, matching spectrum. Since we observe the free ring hydroxyl stretch in all the IR−UV double resonance spectra, hydrogen bonding of the ring hydroxyl, which could freeze it in one position, can be eliminated. Therefore the more likely explanation is that the band origins are so close together that they are unresolvable by our experimental method. For this spectrum, the frequencies and intensities calculated for structures 1a and 1b exhibit the best fit. These two structures, as shown in Figure 4, are predicted to be the lowest in energy. We observe just one spectrum, both in the UV and in the IR, for these structures, and at this level of experiment we cannot distinguish between them. It is possible that rotational spectroscopy could reveal the orientation of the phenolic hydroxyl group, assuming that both conformers are actually present and can be separated from each other. In spectrum E, the carboxylic hydroxyl stretch is shifted further to the red compared

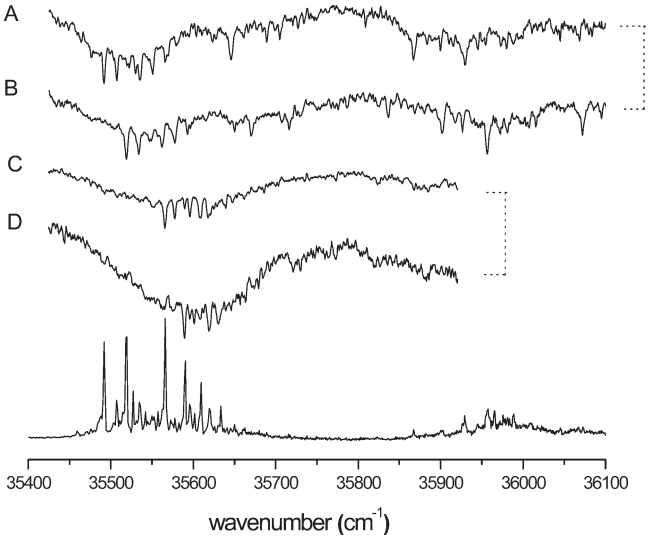

Figure 6. R2PI spectrum (bottom trace) and the UV−UV double resonance spectra of YG showing four different conformers for this molecule.

to that in spectra A and C, which indicates that this hydroxyl is involved in a stronger hydrogen bond than is the hydroxyl in the conformers for A and C. We observe this peak to be very broad, and that its maximum is around 3241 cm^{-1}, while the calculations for structures 1a and 1b predict this mode to appear at 3282 cm^{-1}.

Spectra F and G are similar to B and D, in which the phenolic hydroxyl is free. The only difference is that for F and G the NH_2 antisymmetric mode is red-shifted by about 20 cm^{-1} to 3414 cm^{-1}. Structures 4a and 4b have best fit to this pair.

II. Tyrosine-Glycine (YG). Figure 6 shows the R2PI spectrum (bottom trace) and the UV−UV double resonance spectra (top traces) for YG. The origin region for this molecule lies in nearly the same spectral range as that of tyrosine. While for tyrosine the red-most origin lies at 35483 cm^{-1}, the red-most origin for YG appears at 35492 cm^{-1}. UV−UV hole burning reveals four different conformations. Similarly to the tyrosine spectra, these spectra can be grouped in pairs. Spectra A and B are the first pair, while C and D form the second pair. As the IR−UV data will show, all of these belong to conformers, in which the hydroxyl on the aromatic ring is free.

Figure 7 shows the 12 lowest energy structures obtained by DFT (6-31G**). These 12 structures also form six pairs in which the members of each pair differ only in the orientation of the phenolic hydroxyl group. These structures are of three different types: (I) Structures 1a and 1b, which have the lowest energy, are of the first type, in which the carboxylic hydroxyl group exhibits an intramolecular hydrogen bond with the carbonyl of the amide. (II) In the second type, the structure is open and there is no hydrogen bonding. Structures 2a, 2b, 3a, 3b, 4a, 4b, 6a and 6b all belong to this type. (III) In the third type of structure, which includes 5a and 5b, the carboxylic hydroxyl forms a hydrogen bond with the nitrogen of the amide, and the chain is folded so that the carboxyl group is oriented toward the ring. Toroz and van Mourik found similar families of structures.[36] Their conformers 1 and 3 in ref 37 correspond to structures 1a,b. Twelve of the 20 conformers in that work, denoted by "OHO", are of type I. Conformer pairs (11,12) and (10,7) in ref 37 roughly correspond to structures 4a,b and 3a,b, respectively; conformers 6 and 4 correspond to structures 6a,b.

Figure 8a shows the IR−UV double resonance spectra of the four different conformers. As we observed for tyrosine, the IR spectra for

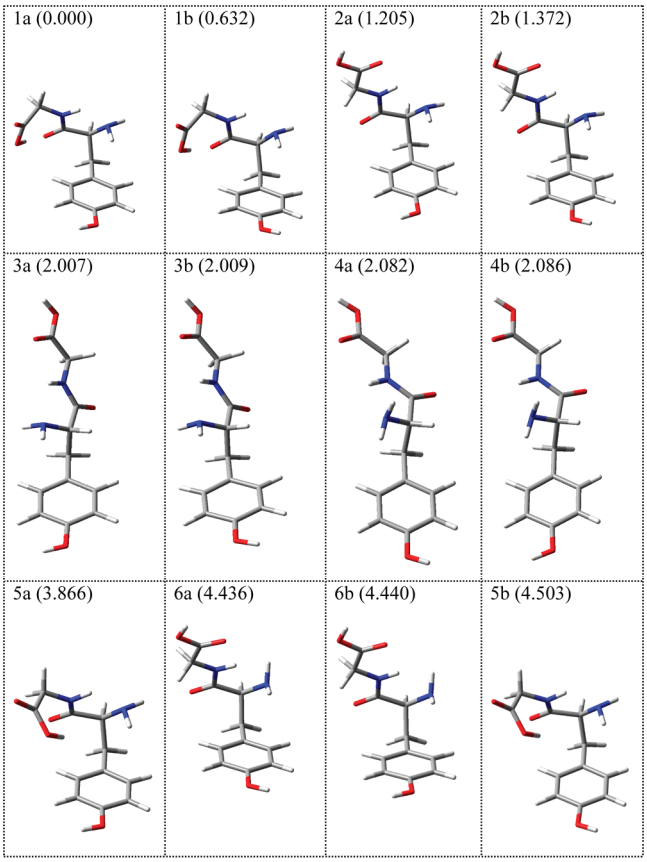

Figure 7. The 12 lowest-energy structures of YG calculated by DFT (6-31G**). The relative energy in kcal/mol is listed above each structure.

each pair with identical UV spectra are also identical. From these spectra we can determine that both the phenolic and the carboxylic hydroxyl groups are free; their stretching modes appear at 3669 cm^{-1} and 3599 cm^{-1}, respectively, which is typical for the free hydroxyl. Therefore, we can exclude the first pair (1a and 1b) and the fifth pair (5a and 5b) as candidate structures, because in these pairs the carboxylic hydroxyl participates in a hydrogen bond. The amide NH stretch appears at 3421 cm^{-1} in all the spectra, and the only difference between the pairs of spectra is where the NH_2 symmetric and antisymmetric stretches appear. This suggests that the structures associated with each pair are similar, except for the orientation of the NH_2 group.

Figure 8b shows the calculated frequencies for the structures in Figure 7. As we noted above, the only candidate pairs are those of type II in which the carboxylic hydroxyl group is free, or (2a,2b), (3a,3b), (4a,4b), and (6a,6b). By comparing the frequency of the amide NH stretch calculated for these four pairs with the experimental frequency, we can also exclude the pair (6a,6b). For this pair, the calculated frequency is 3483 cm^{-1}, the blue-shift perhaps due to a repulsive interaction between the amide hydrogen and the two hydrogens on the amino group. For the remaining three pairs [(2a,2b), (3a,3b), (4a,4b)], the calculated frequency for this mode matches the experimental frequency to within 4 cm^{-1}. These three structures and their frequencies are very similar, so the precise assignment can only be tentative and will be based on the shifting in the bands for NH_2 symmetric stretching mode. In spectra A and B, this moderately weak band appears at 3358 cm^{-1}, and in spectra C and D, it appears at 3349 cm^{-1}. The calculated frequencies of this mode for the pairs

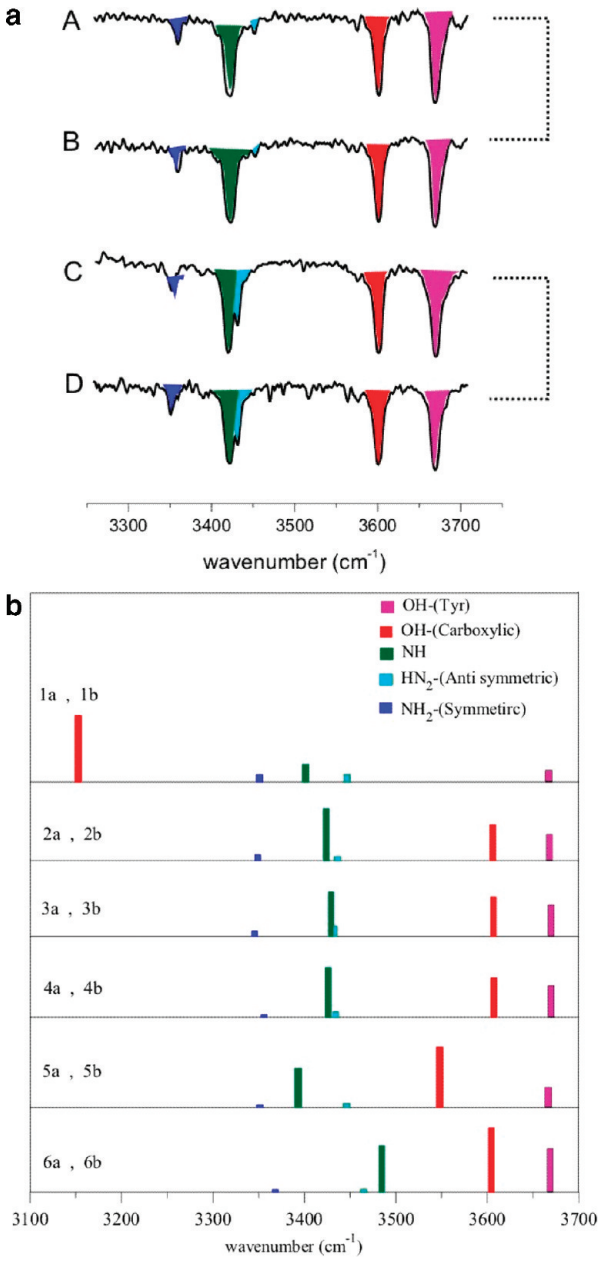

Figure 8. (a) The IR−UV double resonance spectra for the four conformers of YG observed by UV−UV double resonance spectroscopy in Figure 6. Peaks are color coded according to assignments as discussed in the text. Color coding is identical to that in panel b. (b) The calculated spectra for the 12 structures from Figure 7. The frequencies were scaled by a factor of 0.9602.

(3a,3b) and (4a,4b), which are 3346 cm^{-1}, and 3356 cm^{-1}, respectively, are closest to the experimental frequencies. Therefore, we can tentatively assign spectra A and B to the pair (4a,4b), and spectra C and D to (3a,3b).

We note that for tyrosine we observe three structures in which the carboxylic hydroxyl group is hydrogen bonded, whereas for YG we observe no such structures. For comparison, we also studied the protected amino acid tyrosine ethyl ester, in which the glycine is replaced by an ethyl group. By thus blocking the C terminus of the tyrosine, we prevent the aforementioned intramolecular hydrogen bonding, and therefore all the conformers that exhibit such interaction are not possible anymore. Figure 9 shows the R2PI spectrum

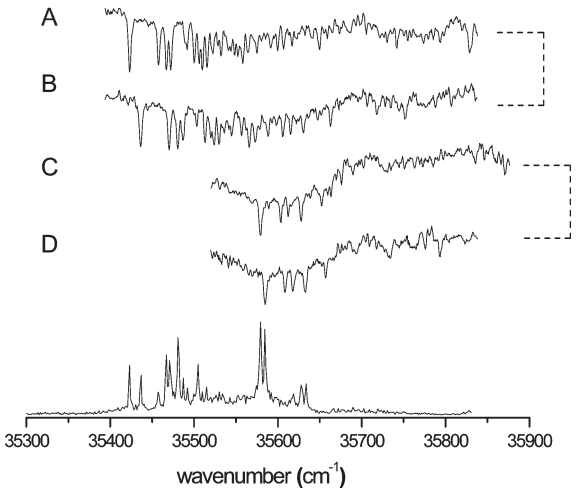

Figure 9. R2PI spectrum (bottom trace) and the UV−UV double resonance spectra of tyrosine ethyl ester. The UV−UV spectra show behavior similar to that of YG.

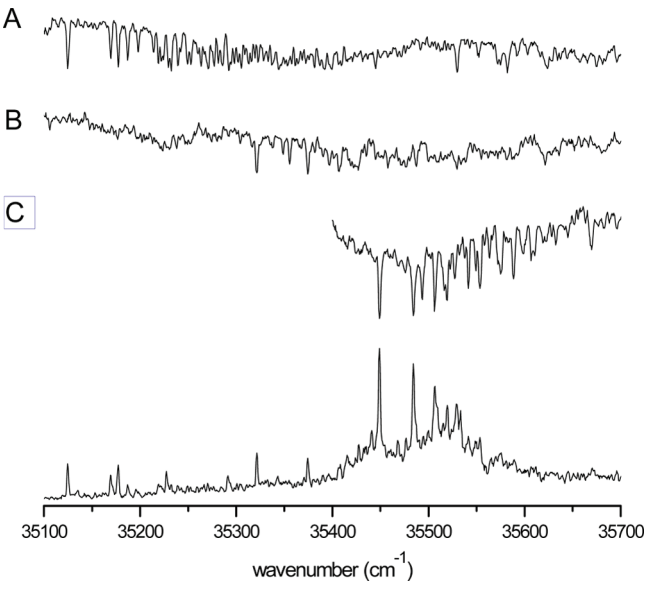

Figure 10. R2PI spectrum (bottom trace) and the UV−UV double resonance spectra of YGG.

(bottom trace) and the UV−UV double resonance spectra (top traces) of tyrosine ethyl ester. As was the case for the dipeptide YG, we observe four different structures, which also belong to the first class of conformations, that is, those that can be grouped in pairs having two orientations of the ring hydroxyl group. Spectra A and B belong to the first pair, and spectra C and D belong to the second pair. Apparently, the glycine in the dipeptide YG acts as a blocking group in similar fashion to the ethyl group in tyrosine ethyl ester. The carboxyl group in YG is not available for interaction by structural constraints because the dipeptide chain is too short to effectively fold back.

B3LYP calculations predict extended conformations to be more stable, whereas MP2 calculations favor folded structures by incorporating dispersion. Toroz and van Mourik predict a more than 350 cm^{-1} redshift for all "book" conformations.[36] They also show that it is difficult to obtain reliable structures and relative energies for YG with either B3LYP or MP2 (with a small

dx.doi.org/10.1021/jp110601w |J. Phys. Chem. A 2011, 115, 6077–6087

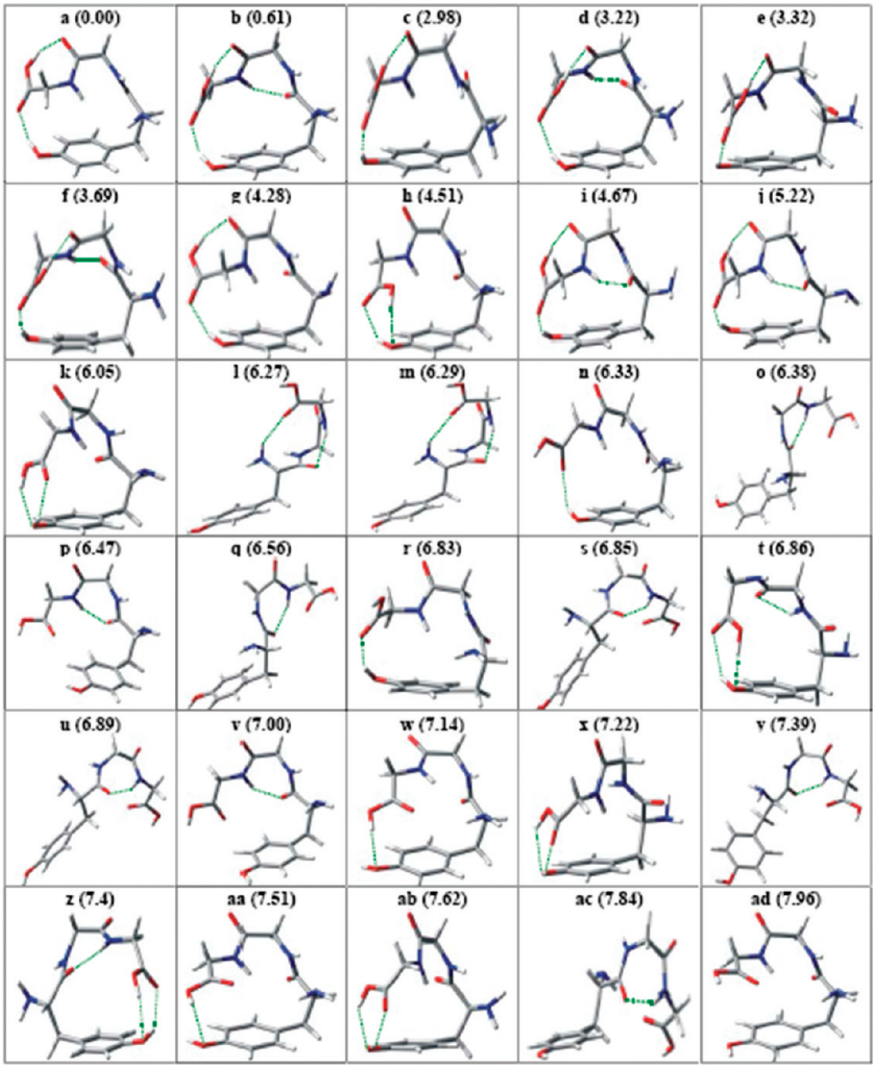

Figure 11. The 30 lowest-energy structures of YGG calculated by DFT (6-31G**). The relative energy in kcal/mol is listed above each structure.

to medium-sized basis set): B3LYP misses conformers due to lacking dispersion, whereas MP2 misses conformers due to large intramolecular BSSE effects.[37,38] We find only the stretched conformations, evidenced by the observation that the carboxyl OH is totally free in both pairs.

III. Tyrosine-Glycine-Glycine (YGG). Figure 10 shows the R2PI spectrum (bottom trace) and the UV−UV double resonance spectra of the tripeptide YGG. Compared to tyrosine, this molecule is much more complex. Despite this increased complexity, the number of observed conformations in this jet-cooled experiment decreases from seven to only three. Compared to the red-most origin of tyrosine, the origin in spectrum A for YGG is shifted to the red by about 360 cm^{-1}, and the origin in spectrum B is shifted about 162 cm^{-1} to the red. The origin in spectrum C appears in almost the same place as the red-most origin for tyrosine. It is remarkable that the three conformers associated with these spectra are completely different from each other. That is, no two form a pair in which the only difference between them is the orientation of the ring hydroxyl group as in the earlier cases. This can be explained by the fact that YGG is long enough to make interaction between the C terminus and the hydroxyl of the phenol ring possible. In this case, the hydroxyl of the phenol is restricted to one position.

From 80 different structures, fully optimized at the DFT (6-31G**) level, we selected the 30 lowest energy structures. Figure 11 shows these 30 structures. On the basis of the intermolecular hydrogen bonding that different structures display, we can categorize these structures into three different groups or families of structures: (I) In the first group, the phenolic hydroxyl displays a hydrogen bond with the carbonyl of the carboxylic group, and the carboxylic hydroxyl interacts with the oxygen of the second amide ("2" in Figure 1). This group includes the structures a−g, i, and j. Some of these structures (b, d, f, i, and j) display a γ-turn. This is a feature in which the carbonyl of amide 1 interacts with the H of amide 2. (II) In the second group, the carboxylic group exhibits intermolecular hydrogen bonding only with the phenolic hydroxyl group. This set contains the structures h, k, n, r, t, w, x, z, aa, and ab. (III) In the third group, both hydroxyls (phenolic and carboxylic) are free. This group contains the structures l, m, o, p, q, s, u, v, y, ac, and ad. While the UV−UV hole burning spectroscopy shows three different conformers, the calculations predict that at least some structures in which the ring hydroxyl group is free should appear in pairs analogous to those for Y and for YG. For example, structures l and m are a pair, as are structures o and q. Toroz and van Mourik performed calculations at the HF/3-21G*, B3LYP/6-31+G*, and MP2/6-31+G* levels and also found three families of structures, similar to those reported here, however, with different

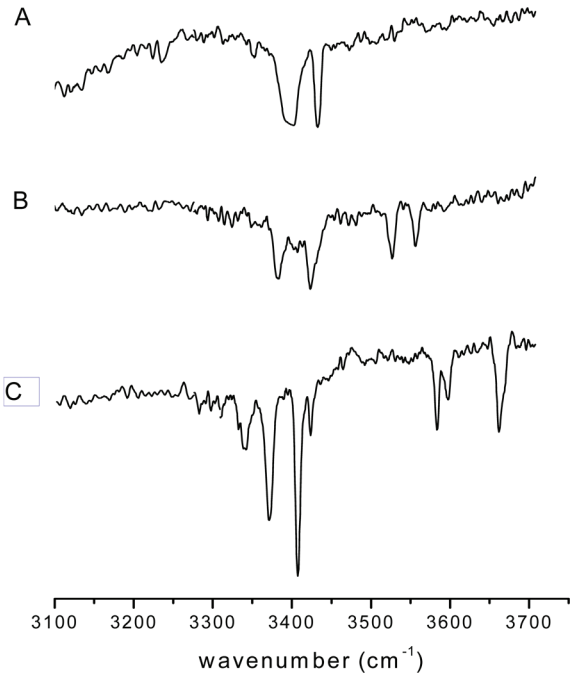

Figure 12. The IR−UV double resonance spectra for the three conformers of YGG observed by UV−UV double resonance spectroscopy in Figure 10. Peaks are color coded according to assignments as discussed in the text. Color coding is identical to that in Figure 13.

relative energies and different detailed structures within each family.[33] We will compare the computed frequencies from those calculations with our findings below.

Figure 12 shows the IR−UV double resonance spectra of the three conformers of YGG. In spectrum A, the peaks for the free hydroxyl stretches (phenolic and carboxylic) are missing, and we observe a broad peak at about 3400 cm^{-1} and the onset of a broad absorption at around 3200 cm^{-1} and below, which indicates that both hydroxyls are involved in hydrogen bonding. These features correspond to a structure of type I. In spectrum B, we observe two peaks, at 3527 cm^{-1} and 3556 cm^{-1}, shifted slightly to the red of where those for the free ring and carboxylic hydroxyl stretches normally appear. We therefore expect the conformer for this spectrum to exhibit some hydrogen bonding of both the ring and carboxylic hydroxyl groups, but less than that for the conformer in spectrum (A). These features correspond to a structure of type II. In spectrum C, sharp peaks appear at 3583 cm^{-1} and 3662 cm^{-1}, corresponding to the free carboxylic and ring hydroxyl stretches, respectively. These features correspond to a structure of type III. The peak at 3583 cm^{-1} is red-shifted from its normal position by about 7 cm^{-1}, and there is an additional, smaller peak at 3597 cm^{-1}. This may be the result of a Fermi resonance between the carboxylic hydroxyl stretch and the second overtone of one of the carbonyl stretches, as has been observed in cyclo(phe-ser) for one of the N−H stretches.[39]

Once again, the differentiation of the structures within each family is more subtle. We can only tentatively assign each of the three spectra to a structure within each of their respective families as follows.

Figure 13a shows the IR−UV double resonance spectrum A, with the calculated spectra for the first group of conformers (a-g, i, and j) below it. As is indicated by the red-shift of their amide 2 N−H stretches, structures B, D, F, I, and J possess a γ-turn. Since we do not observe this in the spectrum, we can eliminate these as candidates. Of the four remaining structures, A and C match the IR−UV data best. In these conformers, the ring hydroxyl group is strongly hydrogen bound to the carbonyl of the carboxyl group, and the hydroxyl of the carboxyl group interacts even more strongly with the carbonyl of amide 2.

In figure 13b we show the IR−UV double resonance spectrum B, with the spectra calculated for the second set of conformers (h, k, n, r, t, w, x, z, aa, and ab) below it. As we noted above, this spectrum indicates that both hydroxyl groups are weakly hydrogen bonded, with the ring hydroxyl slightly more strongly bound than that on the carboxyl group. The calculated spectrum that best matches the pattern in spectrum B is that for conformer n. In this conformer, the hydroxyl group on the ring interacts weakly with the carbonyl of the carboxylic group, while the hydroxyl on the carboxylic group is free. Because of the hydrogen bonding of the carbonyl, however, we do observe a small red-shift of the band for the carboxylic hydroxyl stretch.

Figure 13c shows the IR−UV double resonance spectrum C, with the calculated spectra for the third group of conformers (l, m, o, p, q, s, u, v, y, ac, and ad) below it. As both the optimized structures and calculated frequencies indicate, all of these conformers exhibit a γ-turn, except for structure ad. On the basis of the ordering of the four NH and NH_2 stretch bands, we can exclude conformers o, p, q, s, u, and v. In y, the NH_2 bands are missing. This leaves conformers l, m, and ac, of which ac is clearly the best match.

Figure 14 shows the a comparison of the experiment (top trace in each panel) with the frequencies from best matching conformations selected above (middle spectrum in each panel) and the best fitting calculated spectra from the study by Toroz and van Mourik (bottom spectrum in each panel). Although the structures differ in detail, the frequencies agree qualitatively very well.

4. DISCUSSION

Tyrosine and YG exhibit a cluster of origins in a similar spectral region, and for YGG there is an additional set of peaks appearing significantly to the red of this region. In tyrosine and in YG, the ring hydroxyl group is free, as the IR−UV double resonance spectra show. For the YGG conformer with the origin near those for tyrosine and YG (labeled C), this hydroxyl group is also free. For the next YGG conformer to the red (B), this group is weakly hydrogen bound, and for the red-most origin (A), this hydroxyl is strongly hydrogen bound. We associate the degree to which the origin is red-shifted with the strength of the hydrogen bond in which the ring hydroxyl group participates. In this situation, this hydroxyl group acts as a proton donor, and we also associate this red-shift with an increase in electron density in the ring.

In making our assignment, we noticed that for tyrosine, we were able to match with the origins a set of conformers that were calculated to have the lowest energies. For YG, however, the two lowest energy structures did not agree with the spectroscopic evidence. The difference in energy between these structures and the ones we chose is on the order of only 2 kcal/mol, and it is quite possible that higher level calculations would place these structures in a different order. This also applies for YGG, in which case for conformer A we chose the lowest energy structure in the given family of structures, but for conformers B and C, we cannot. Here, the energy difference between the structures having the lowest and the highest energies within the family is around 8 kcal/mol. Because of the complexity of the potential surface for YGG, which arises from the large number of degrees of freedom

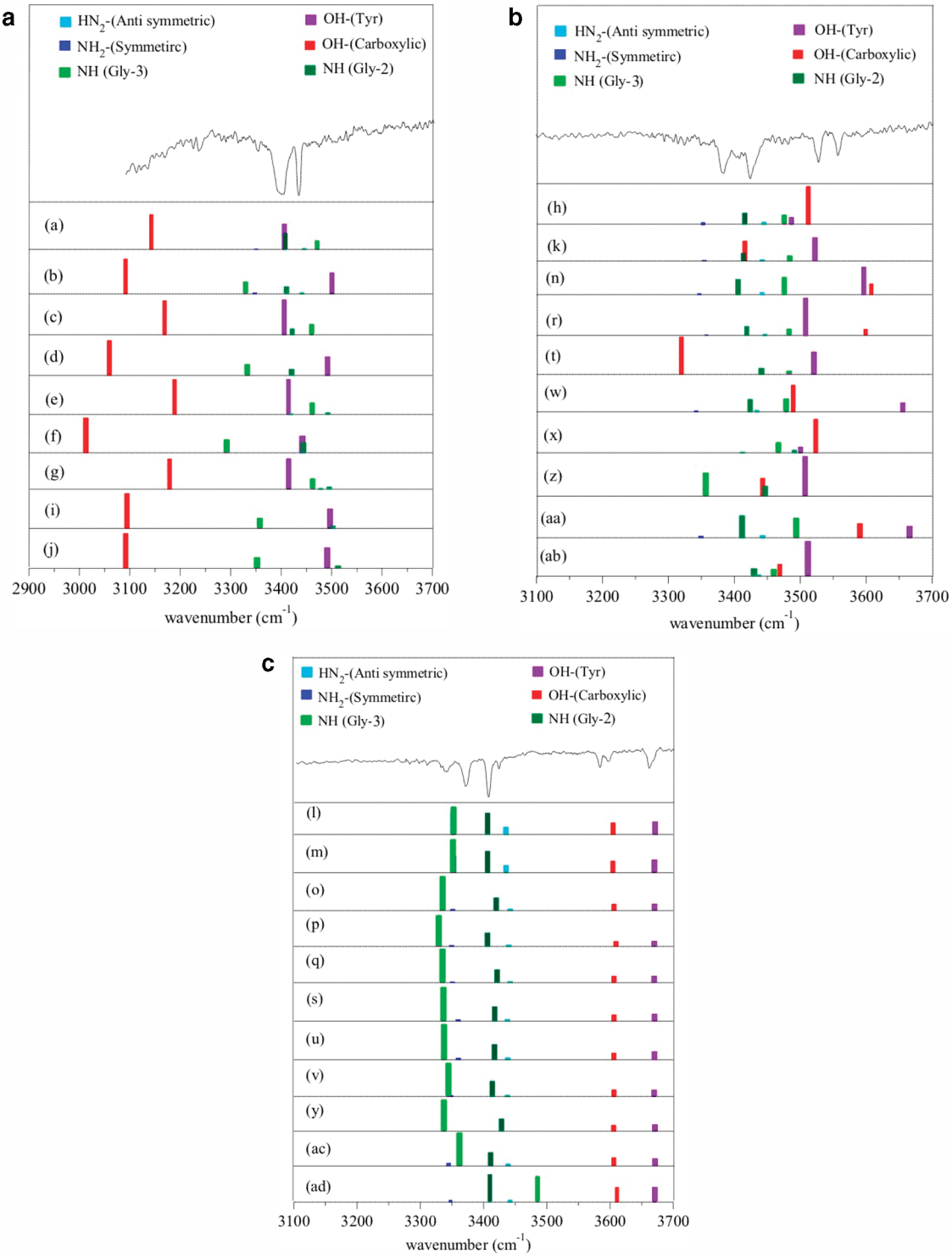

Figure 13. (a) IR−UV double resonance spectrum A from Figure 12, with the calculated spectra for the nine conformers belonging to the structural group associated with it. (b) IR−UV double resonance spectrum B from Figure 12, with the calculated spectra for the 10 conformers belonging to the structural group associated with it. (c) IR−UV double resonance spectrum C from Figure 12, with the calculated spectra for the 11 conformers belonging to the structural group associated with it.

for this molecule, DFT calculations yield many possible structures. By comparing the results of frequency calculations with the experimentally obtained spectra, we are able to eliminate most but not all of these, and we can choose with some confidence those remaining that best match the experiment. Also if we follow the higher level calculations from Toroz and van Mourik we can find a reasonable match with several of their calculated spectra those do not match the lowest energy structures. We find the best match with these calculations for structures (5−7), 12.8−13.4 kcal/mol above the global minimum. One possible conclusion is

dx.doi.org/10.1021/jp110601w |J. Phys. Chem. A 2011, 115, 6077–6087

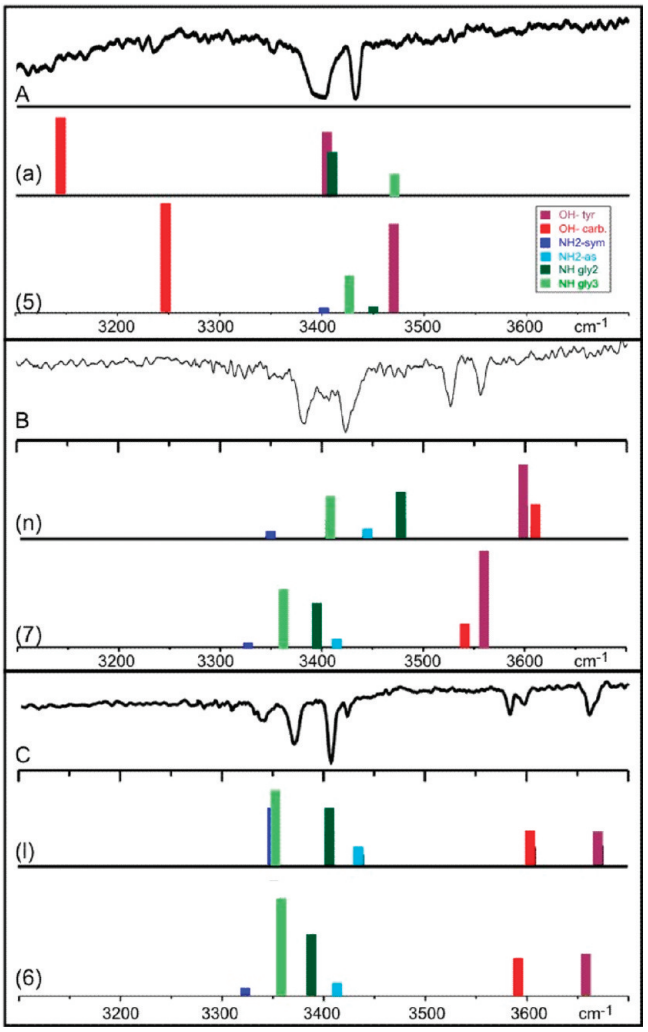

Figure 14. Comparison of the experimental YGG IR-UV spectra (top trace in each panel) with the frequencies from best matching calculated conformations from this work (middle spectrum in each panel) and from the study by Toroz and van Mourik (bottom spectrum in each panel).

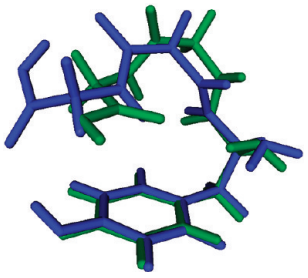

Figure 15. Comparison of lowest energy structures of YGG from the study by Toroz and van Mourik[33] with the lowest energy structure of FGG from Reha et al.[10].

that yet higher level calculations are required to obtain the correct order of energies. It is also possible that we do not observe the lowest energy conformers in these experiments due to a very short excited state lifetime, as proposed by Shemesh et al. in the case of FGG[40] and of WG.[41]

For tyrosine, YG, and YGG, we observe seven, four, and three conformers, respectively. In tyrosine, the ability of the carboxylic hydroxyl group to interact with the lone pair on the amino group gives rise to conformers that would otherwise not exist. In YG, this interaction cannot take place, and so the number of stable conformers decreases. Intramolecular hydrogen bonding through the peptide backbone can lead to secondary features such as tight turns, and these may provide a path for relaxation of the peptide to its global energy minimum. Apparently a dipeptide is too short for this type of hydrogen bonding to occur, requiring at least two peptide bonds in the molecule. That is, the molecule must be a tripeptide or longer, so that a γ-turn is possible. In YGG we observe such a feature in the structure assigned to conformer C, which also exhibits the most intense origin. The ability of YGG to form this turn may play a role in limiting the number of conformations available to it. In addition, interactions that would freeze the ring hydroxyl group in one position would also limit the number of conformers. This is likely for the two conformers that do not exhibit the γ-turn, but in which the ring hydroxyl is bound to some extent (A and B). What remains a puzzle is why the conformer with the γ-turn should not exhibit a pair of origins corresponding to two positions of the ring hydroxyl group.

Another interesting feature of the YGG data is that for conformer A, the UV−UV hole burning spectrum shows considerable vibronic activity that is not evident in the R2PI spectrum. A possible explanation is an additional electronic state lying roughly 100 cm^{-1} above S_1, which is short-lived and decays either to a metastable state above S_0 or to the ground state of a different conformer. If the molecule were to cross over to this state upon excitation, this might make R2PI impossible, but could still deplete the ground state so as to yield sharp peaks in the UV−UV double resonance spectrum. This phenomenon has been observed before, and also with molecules that exhibit a broad R2PI signal but a sharp IR−UV signal.

The only difference between FGG and YGG is the hydroxyl moiety on the phenyl ring in the case of tyrosine. Figure 15 shows a comparison between the most stable folded structures for each of these tripeptides. In the case of FG, the stabilizing force is the dispersive force between the C-terminus and the π cloud on the phenyl ring; in the case of YGG, the stabilization results from the hydrogen bonding of the C-terminus with the OH on the ring. Remarkably, in both cases the folded structure of the backbone is virtually identical. These model systems may represent the beginnings of peptide folding, which should be further explored by studying larger peptides by similar methods to those shown here.

Present Addresses

[§]Weizmann Institute of Science, Rehovot 76100, Israel.
[∥]Department of Physics, University of California, Santa Barbara, CA 93106.
[⊥]Millennium Laboratories, San Diego, CA 92127.
[#]NASA Goddard Space Flight Center, 8800 Greenbelt Road, Greenbelt, MD 20771.

■ ACKNOWLEDGMENT

This work is supported by the National Science Foundation under CHE-0911564.

■ DEDICATION

This paper is dedicated to the memory of Victoria Buch, whose insights both in science and in social issues continue to serve as a lasting inspiration.

REFERENCES

(1) Zwier, T. S. *J. Phys. Chem. A* **2001**, *105*, 8827.
(2) Snoek, L. C.; Kroemer, R. T.; Simons, J. P. *Phys. Chem. Chem. Phys.* **2002**, *4*, 2130.
(3) Simons, J. P. *C. R. Chim.* **2003**, *6*, 17.
(4) Vaden, T. D.; Gowers, S. A. N.; de Boer, T. S. J. A.; Steill, J. D.; Oomens, J.; Snoek, L. C. *J. Am. Chem. Soc.* **2008**, *130*, 14640.
(5) Gloaguen, E.; Valdes, H.; Pagliarulo, F.; Pollet, R.; Tardivel, B.; Hobza, P.; Piuzzi, F.; Mons, M. *J. Phys. Chem. A* **2010**, *114*, 2973.
(6) Chin, W.; Dognon, J. P.; Piuzzi, F.; Tardivel, B.; Dimicoli, I.; Mons, M. *J. Am. Chem. Soc.* **2005**, *127*, 707.
(7) Cohen, R.; Nir, E.; Grace, L. I.; Brauer, B.; de Vries, M. S. *J. Phys. Chem. A* **2000**, *104*, 6351.
(8) Abo-Riziq, A.; Crews, B. O.; Callahan, M. P.; Grace, L.; de Vries, M. S. *Angew. Chem., Int. Ed.* **2006**, *45*, 5166.
(9) Abo-Riziq, A.; Bushnell, J. E.; Crews, B.; Callahan, M.; Grace, L.; De Vries, M. S. *Chem. Phys. Lett.* **2006**, *431*, 227.
(10) Reha, D.; Valdes, H.; Vondrasek, J.; Hobza, P.; Abu-Riziq, A.; Crews, B.; de Vries, M. S. *Chemistry—Eur. J.* **2005**, *11*, 6803.
(11) Abo-Riziq, A. G.; Bushnell, J. E.; Crews, B.; Callahan, M. P.; Grace, L.; De Vries, M. S. *Int. J. Quantum Chem.* **2005**, *105*, 437.
(12) Snoek, L. C.; Robertson, E. G.; Kroemer, R. T.; Simons, J. P. *Chem. Phys. Lett.* **2000**, *321*, 49.
(13) Rizzo, T. R.; Park, Y. D.; Peteanu, L.; Levy, D. H. *J. Chem. Phys.* **1985**, *83*, 4819.
(14) Snoek, L. C.; Kroemer, R. T.; Hockridge, M. R.; Simons, J. P. *Phys. Chem. Chem. Phys.* **2001**, *3*, 1819.
(15) Rizzo, T. R.; Park, Y. D.; Peteanu, L. A.; Levy, D. H. *J. Chem. Phys.* **1986**, *84*, 2534.
(16) Philips, L. A.; Webb, S. P.; Martinez, S. J.; Fleming, G. R.; Levy, D. H. *J. Am. Chem. Soc.* **1988**, *110*, 1352.
(17) Martinez, S. J.; Alfano, J. C.; Levy, D. H. *J. Mol. Spectrosc.* **1991**, *145*, 100.
(18) Martinez, S. J.; Alfano, J. C.; Levy, D. H. *J. Mol. Spectrosc.* **1992**, *156*, 421.
(19) Chin, W.; Dognon, J. P.; Canuel, C.; Piuzzi, F.; Dimicoli, I.; Mons, M.; Compagnon, I.; von Helden, G.; Meijer, G. *J. Chem. Phys.* **2005**, 122.
(20) Chin, W.; Compagnon, I.; Dognon, J. P.; Canuel, C.; Piuzzi, F.; Dimicoli, I.; von Helden, G.; Meijer, G.; Mons, M. *J. Am. Chem. Soc.* **2005**, *127*, 1388.
(21) Unterberg, C.; Gerlach, A.; Schrader, T.; Gerhards, M. *J. Chem. Phys.* **2003**, *118*, 8296.
(22) Gerhards, M.; Unterberg, C.; Gerlach, A.; Jansen, A. *Phys. Chem. Chem. Phys.* **2004**, *6*, 2682.
(23) Fricke, H.; Gerlach, A.; Unterberg, C.; Rzepecki, P.; Schrader, T.; Gerhards, M. *Phys. Chem. Chem. Phys.* **2004**, *6*, 4636.
(24) Hunig, I.; Kleinermanns, K. *Phys. Chem. Chem. Phys.* **2004**, *6*, 2650.
(25) Hünig, I.; Seefeld, K. A.; Kleinermanns, K. *Chem. Phys. Lett.* **2003**, *369*, 173.
(26) Bakker, J. M.; Plutzer, C.; Hunig, I.; Haber, T.; Compagnon, I.; von Helden, G.; Meijer, G.; Kleinermanns, K. *ChemPhysChem* **2005**, *6*, 120.
(27) Li, L.; Lubman, D. M. *Appl. Spectrosc.* **1989**, *43*, 543.
(28) Li, L.; Lubman, D. M. *Appl. Spectrosc.* **1988**, *42*, 418.
(29) Grace, L. I.; Cohen, R.; Dunn, T. M.; Lubman, D. M.; de Vries, M. S. *J. Mol. Spectrosc.* **2002**, *215*, 204.
(30) Cohen, R.; Brauer, B.; Nir, E.; Grace, L.; de Vries, M. S. *J. Phys. Chem. A* **2000**, *104*, 6351.
(31) Valdes, H.; Reha, D.; Hobza, P. *J. Phys. Chem. B* **2006**, *110*, 6385.
(32) Cable, J. R.; Tubergen, M. J.; Levy, D. H. *J. Am. Chem. Soc.* **1987**, *109*, 6198.
(33) Toroz, D.; van Mourik, T. *Mol. Phys.* **2007**, *105*, 209.
(34) Meijer, G.; Devries, M. S.; Hunziker, H. E.; Wendt, H. R. *Appl. Phys. B: Photophys. Laser Chem.* **1990**, *51*, 395.
(35) Snoek, L. C.; Robertson, E. G.; Kroemer, R. T.; Simons, J. P. *Chem. Phys. Lett.* **2000**, *321*, 49.
(36) Toroz, D.; Van Mourik, T. *Mol. Phys.* **2006**, *104*, 559.
(37) Holroyd, L. F.; van Mourik, T. *Chem. Phys. Lett.* **2007**, *442*, 42.
(38) Shields, A. E.; van Mourik, T. *J. Phys. Chem. A* **2007**, *111*, 13272.
(39) Abo-Riziq, A. G.; Crews, B.; Bushnell, J. E.; Callahan, M. P.; De Vries, M. S. *Mol. Phys.* **2005**, *103*, 1491.
(40) Shemesh, D.; Sobolewski, A. L.; Domcke, W. *J. Am. Chem. Soc.* **2009**, *131*, 1374.
(41) Shemesh, D.; Hattig, C.; Domcke, W. *Chem. Phys. Lett.* **2009**, *482*, 38.